Appl Nanosci (2016) 6:495–502
DOI 10.1007/s13204-015-0465-z

ORIGINAL ARTICLE

Synthesis, characterisation of polyaniline–Fe_3O_4 magnetic nanocomposite and its application for removal of an acid violet 19 dye

Manohar R. Patil[1] · Subhash D. Khairnar[1] · V. S. Shrivastava[1]

Received: 28 January 2015 / Accepted: 27 May 2015 / Published online: 14 June 2015

Abstract The present work deals with the development of a new method for the removal of dyes from an aqueous solution using polyaniline (PANI)–Fe_3O_4 magnetic nanocomposite. It is synthesised in situ through self-polymerisation of monomer aniline. Photocatalytic degradation studies were carried out for cationic acid violet 19 (acid fuchsine) dye using PANI–Fe_3O_4 nanocomposite in aqueous solution. Different parameters like catalyst dose, contact time and pH have been studied to optimise reaction condition. The optimum conditions for the removal of the dye are initial concentration 20 mg/l, adsorbent dose 6 gm/l, pH 7. The EDS technique gives elemental composition of synthesised PANI–Fe_3O_4. The SEM and XRD studies were carried for morphological feature characteristics of PANI–Fe_3O_4 nanocomposite. The VSM (vibrating sample magnetometer) gives magnetic property of PANI–Fe_3O_4 nanocomposite; also FT-IR analysis gives characteristics frequency of synthesised PANI–Fe_3O_4. Besides the above studies kinetic study has also been carried out.

Keywords PANI–Fe_3O_4 magnetic nanocomposites · Photocatalytic degradation · Acid violet 19 dye · SEM · XRD · VSM

✉ V. S. Shrivastava
drvinod_shrivastava@yahoo.com

Manohar R. Patil
profmanoharpatil@gmail.com

Subhash D. Khairnar
subhashkhairnar20@gmail.com

[1] Nano-Chemistry Research Laboratory, G.T.P. College, Nandurbar 425412, India

Introduction

About 15 % of the total world production of dyes is lost during the dyeing process and is released in the textile effluents (Houas et al. 2001). To reduce the risk of environmental pollution from such textile effluent, it is necessary to treat them to before discharging in environment. (Shrivastava 2012). Photosensitized degradation of coloured contaminants in wastewater on semiconductor surface is crucial (Chatterji 2004; Zhang et al. 2008; Ameta et al. 2014). Among the new oxidation methods or advanced oxidation processes (AOP), heterogeneous photo-catalysis appears as an emerging destruction technology leading to the total mineralisation of most of the organic pollutants (Imanishi et al. 2010).

In present era, the use of semiconductor metal oxides as photo-catalysts for degradation of pollutants has attracted attention of researchers. Semiconductor metal oxide Nanoparticles have been studied due to their novel optical, electronic, magnetic, thermal and mechanical properties and potential application in catalyst, gas sensors and photoelectronics devices (Grätzel 2004; Senadeera et al. 2004). Dyes are not removed by traditional methods such as biological, physical and chemical methods. Nowadays the advanced oxidation process (AOP) is used for the detoxification of contaminated dyes solution (Sato et al. 2004; Patil et al. 2012; Meshram et al. 2011; Tang et al. 2003; Jang et al. 2009). AOP has many advantages as the complete mineralisation of the pollutants are non selective processes can be used low contaminant and can be combined with other methods (del Maria 2013). Advanced oxidation processes are based on generation of reactive species through illumination of UV or solar light of some active materials. This process used to oxidise organic and inorganic pollutants (Aplin and Waite 2003).

Nowadays, ferrite has attracted considerable attention due to its narrowing band gap energy of nearly 2.1 eV (Chen et al. 2007; Singhal et al. 2013). Magnetic nanocomposite has been found to be potential alternative in future for materials with low photocatalytic activity. Degradation of organic pollutants and toxic dyes has been important aspect to study the photocatalytic efficiency of magnetic composites (Wang et al. 2005; Soltani and Entezari 2013).

The present work report is a new and simple method for removal and recovery of Acid violet 19 dye by PANI–Fe_3O_4 Magnetic nanocomposites used as a catalyst. Photocatalytic degradation experiment was carried out and also studied the degradation kinetics of Acid violet 19 on PANI–Fe_3O_4 magnetic nanocomposites.

Photocatalytic mechanism

Based on the results of photocatalytic mechanism under Uv–Visible light irradiation can be proposed as, PANI absorbs UV–Visible light to induce π–π* transition, transporting the excited state electrons to the π* orbital. The d orbital conducting band of Fe_3O_4 is sufficient for transition and have chemical bond interaction according to the mechanism which is shown in the Fig. 1a (Patil and Shrivastava 2014).

Experimental

Materials and methods

Acid violet 19 dye, Fe $(NO_3)_3 9H_2O$, $FeSO_4 \cdot 6H_2O$, NH_4OH, monomer aniline, distilled water, ammonium per-sulphate $[(NH_4)_2S_2O_8]$. The water soluble acid violet 19 dye which has M.F. $C_{20}H_{17}N_3O_9S_3Na_2$, M.W. 585.54 gm

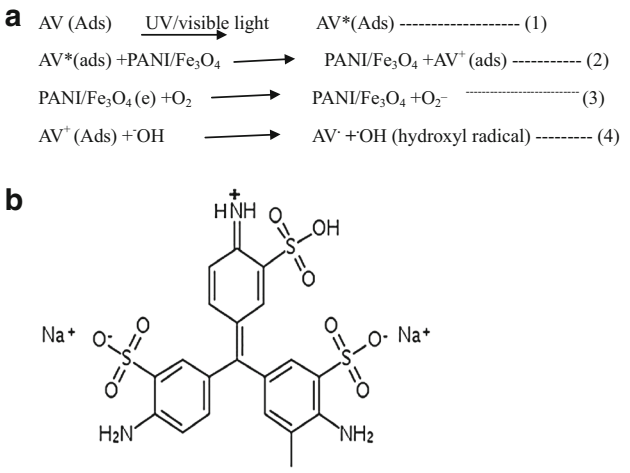

Fig. 1 **a** Photosensitisation effect by the acid violet (AV) 19 Dye. **b** Structure of acid violet 19 dye

and PANI–Fe_3O_4 nanocomposite was used as catalyst. All chemicals and reagents were of analytical grade purity. The structure of dye is presented in the Fig. 1b. The stock solution 1000 mg/l of an acid violet 19 dye was prepared in double distilled water, from which desired conc. of dye solution was prepared. In 50 ml of dye solution of the desired concentration, of different adsorbent dose was added and stirred with magnetic stirrer. At specific time interval suitable aliquot of the sample was withdrawn and analysed after centrifugation. The changes in dye concentration were determined by UV–Visible double beam spectrophotometer (systronics model-2203) at λ max 545 nm in our laboratory.

Instrumentation

The Photocatalytic degradation of acid violet 19 dye was carried out in a Photocatalytic reactor with a 400-W medium pressure Mercury lamp. The reactor consists of a cylindrical Pyrex glass rector, double-walled quartz cooling water jacket to maintain the temperature and prevent the reactor from excessive heating. The reaction solution was stirred with magnetic stirrer at a constant speed. The changes in dye concentration are measured using spectrophotometer (Systronics 2203). The pH metric measurement were made on equip-tronics digital pH meter (Model-E610) fitted with glass electrode which is previously standardized with buffers of known pH in Acidic and basic media.

Preparation of Fe_3O_4 Nanoparticles

Fe_3O_4 magnetic particles were prepared by co-precipitation method. A complete precipitation of Fe_3O_4 was achieved under basic condition, by maintaining molar ratio of $Fe(NO_3)_3 9H_2O$:$FeSO_4 6H_2O$ as 1:2. In this experiment $Fe(NO_3)_3 9H_2O$ and $FeSO_4 6H_2O$ were dissolved in 80 ml distilled water with vigorous magnetic stirring. After stirring, this solution was heated up to 80 °C, then slowly added ammonium hydroxide solution up to pH 11. At this condition complete growth of Fe_3O_4 crystals was observed. The resulting nanoparticles were filtered and repeatedly washed with water and then with ethanol, finally dried at 80 °C in oven for 24 h.

Preparation of PANI–Fe_3O_4 nanocomposite

The solution of Fe_3O_4 Nanoparticle, monomer aniline, and ammonium per-sulphate $((NH_4)_2S_2O_8)$ was prepared in distilled water with vigorous stirring at R.T. The amount of Fe_3O_4 and monomer aniline was taken in 1:2 ratio. The pH value was controlled during the entire experiment up to pH 11. A black precipitate of PANI–Fe_3O_4 was observed after

10 h. The resulting polymer nanocomposite was poured into water and filtered. Each wash step was carried out until the filtrate becomes clear and colourless. Finally, the magnetic polymer nanocomposite was washed with distilled water, ethanol, and then finally dried in oven (El-Mahy et al. 2013).

Results and discussion

Characterisation and analysis

SEM analysis

Scanning electron microscopy is widely used to study the morphological features and surface characteristics of catalyst. The PANI–Fe_3O_4 nanocomposites was analysed by SEM before Fig. 2a and after photocatalytic degradation of acid violet 19 dye is shown in the Fig. 2b. It shows SEM micrographs of PANI–Fe_3O_4 and PANI–Fe_3O_4 after photocatalytic degradation of Acid violet 19 dye. They show surface texture of PANI–Fe_3O_4. The PANI–Fe_3O_4 has heterogeneous surface, there is whitish cluster of Fe_3O_4 nanoparticles on the dark greyish surface of PANI. There is no large difference seen before and after photocatalytic degradation on catalyst surface.

Electron dispersive X-ray spectroscopy (EDS) analysis

EDS can be used to find the chemical composition of materials down to a spot size of a few microns, and to create element composition maps over a much broader raster area. Together, these capabilities provide fundamental compositional information for a wide variety of materials. From the analysis, comes to know that PANI–Fe_3O_4 nanocomposite consists of exact elemental composition of specific element like Fe, O, C, N etc. is as shown in the (Fig. 3). The observed elemental composition is Fe = 3.39 %, O = 16.68 %, C = 67 %, N = 12.21 %. As PANI–Fe_3O_4 is conducting material therefore it needs to coat with gold (Au) metal.

XRD analysis

The XRD diagram of PANI–Fe_3O_4 is as shown in Fig. 4. It shows the main peak spectrum 2θ of 35.03° and 2° peak of 2θ of 42.57° and 64.95°, respectively. The high intensity of peaks indicates the crystalline nature of PANI–Fe_3O_4. The average crystalline size of PANI–Fe_3O_4 particles was estimated by the Scherer formula is 22 nm. It has shown match scan with JCPDS PDF no: 01-078-6086.

FT-IR analysis

The FT-IR spectra of PANI–Fe_3O_4 nanocomposite is shown in Fig. 5. It shows absorption band at 564.13 cm^{-1}, due to Fe–O stretching vibration. There are characteristic peaks of PANI at 1133, 1180, 1600, 1650, 3250 cm^{-1}, due to the C–N stretching vibration band, the C=C stretching vibration in aromatic ring of aniline, and the N–H stretching vibration, respectively. These frequencies indicate the formation of PANI–Fe_3O_4 nanocomposite.

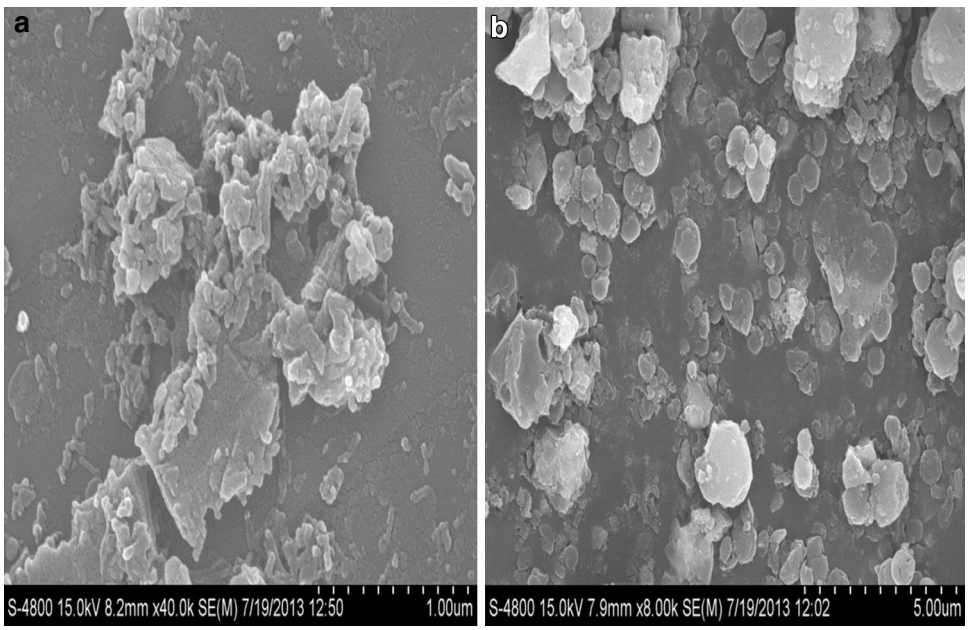

Fig. 2 **a** SEM images of prepared PANI–Fe_3O_4 nanocomposites. **b** SEM images after photocatalytic degradation of acid violet 19 dye on PANI–Fe_3O_4 nanocomposites

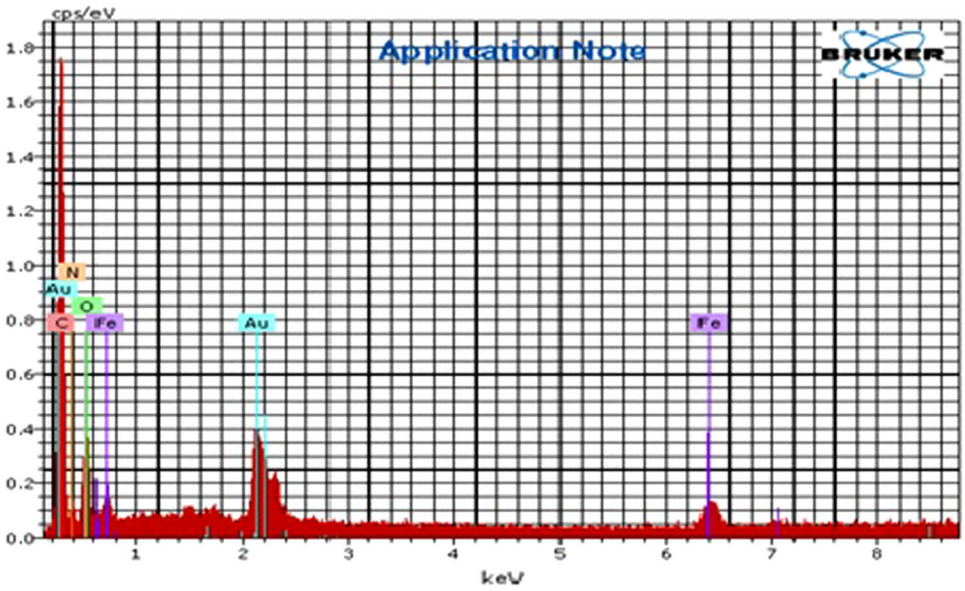

Fig. 3 EDS image of gold coated (Au) PANI–Fe_3O_4 nanocomposites

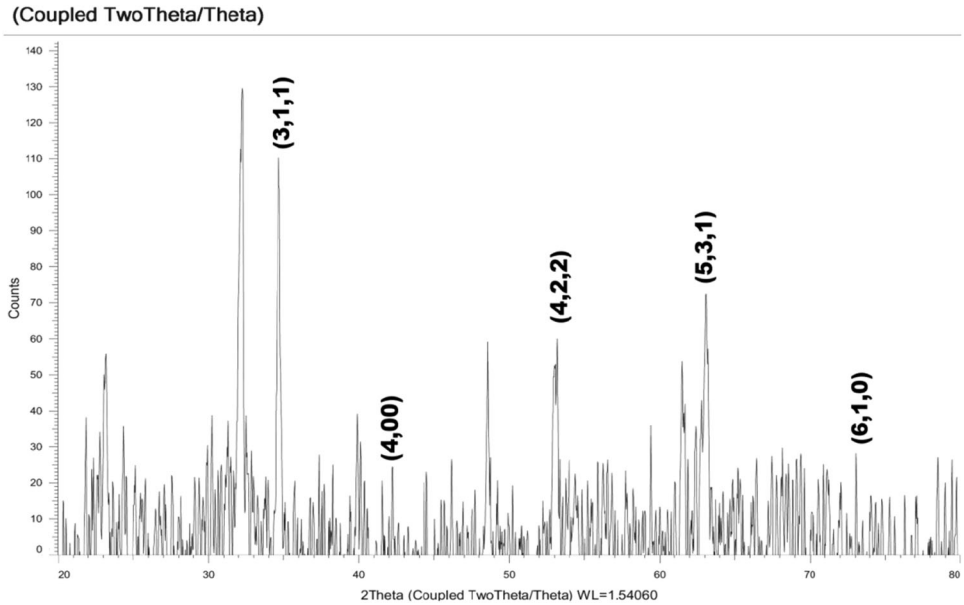

Fig. 4 The XRD diagram of prepared PANI–Fe_3O_4

VSM analysis

The magnetic property of PANI–Fe_3O_4 and Fe_3O_4 were analysed at R.T. by VSM (vibrating sample magnetometer).These nanocomposite magnetic properties were analysed at applied field 10,000 gauss. The Fe_3O_4 nanoparticles show the value of saturation magnetisation is 58.1 emu/g. It is shown in the Fig. 6a. So this magnetisation curve has shown hysteresis loop, which indicates strong ferromagnetic behaviour of Fe_3O_4 nanoparticles. The PANI–Fe_3O_4 nanocomposite has shown the value of saturation magnetisation (Ms) is 400 m emu/g, which is lower than Fe_3O_4. It is shown in the Fig. 6b. So this magnetisation curve of the sample has shown a weak ferromagnetic behaviour, with hysteresis. The magnetic property of nanocomposite is dependent on the sample shape, crystallinity; therefore, it can be adjusted to obtain optimum property.

Parametric studies

The adsorptive removal of acid violet 19 is studied at λ max 545 nm. The optimum condition for removal of dyes is 20 mg/l, pH 7, PANI–Fe_3O_4—6 gm\l. The results obtained during this study are as shown in the Figs. 7, 8, 9.

Effect of catalyst dose

The effect of catalyst dose on the degradation of acid violet is studied by varying different doses of PANI–Fe_3O_4

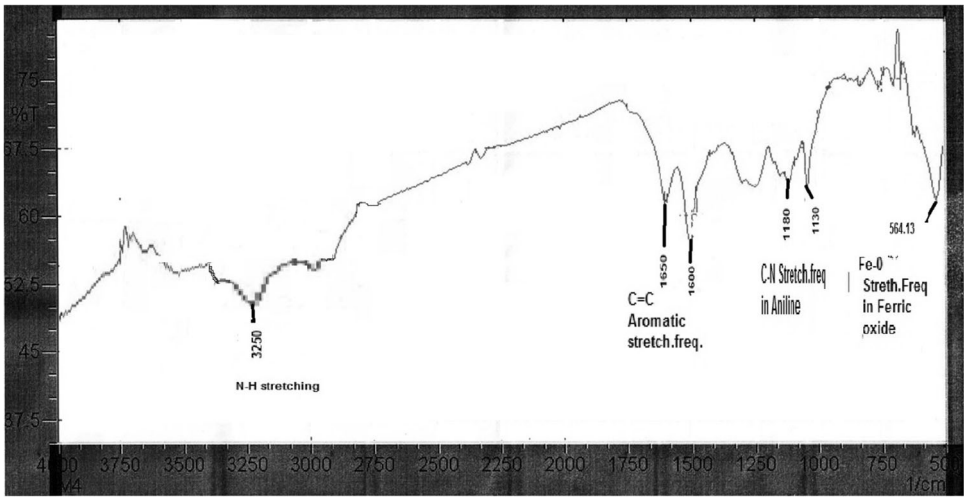

Fig. 5 FT-IR Spectra of synthesised PANI–Fe_3O_4 nanocomposite

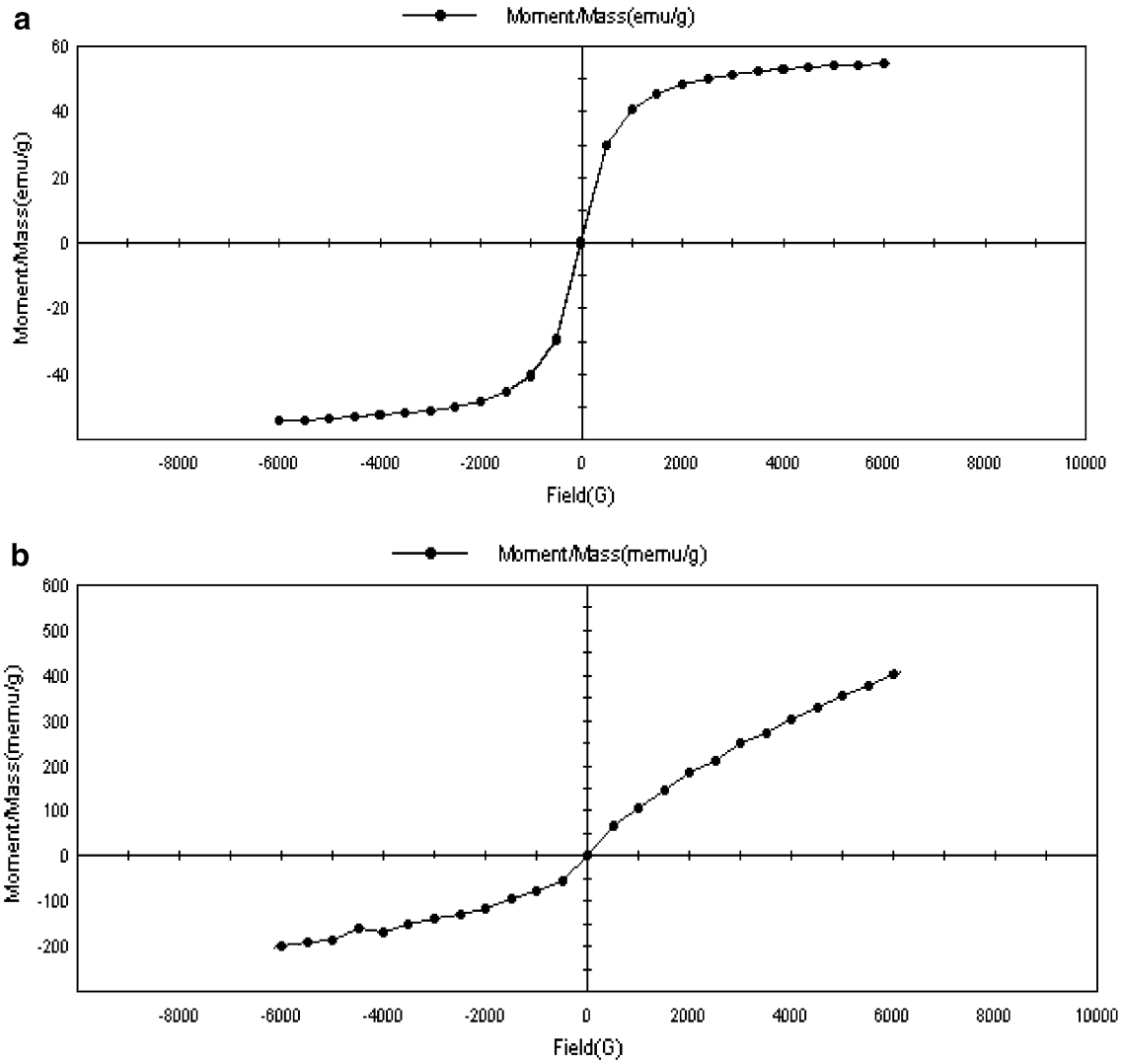

Fig. 6 **a** Magnetisation curve of Fe_3O_4. **b** Magnetisation curve of PANI–Fe_3O_4 nanocomposite

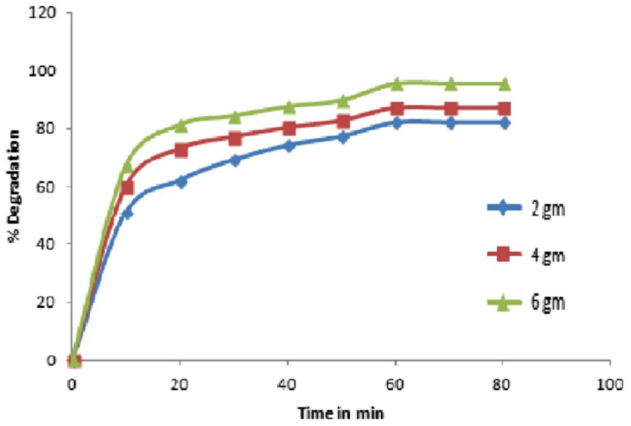

Fig. 7 Effect of catalyst dose on % degradation of acid violet 19 dye for 20 mg/l dye conc. with contact time 80 min, pH 7

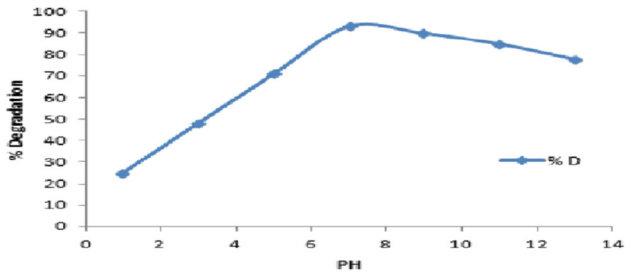

Fig. 8 Effect of pH on removal of acid violet 19 dye by PANI–Fe_3O_4 catalyst dose 6 g/l at 20 mg/l

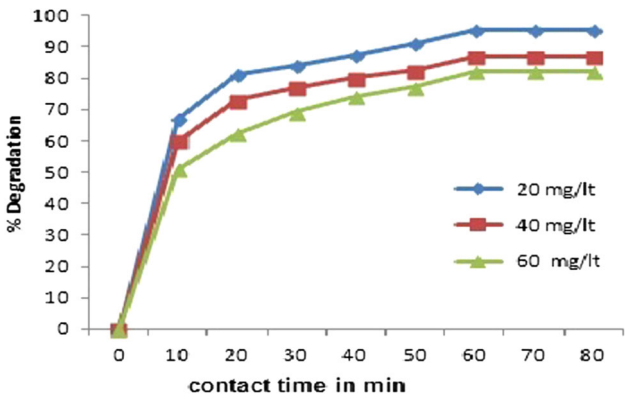

Fig. 9 Effect of contact time of acid violet 19 on % degradation of catalyst dose 6 g\l at pH 7

nanocomposite from 2 to 6 gm\l for 20 mg/l is as shown in Fig. 7. Photocatalytic degradation of acid violet is increased from 82.1 to 95.2 with an increasing amount of PANI–Fe_3O_4 from 2 to 6 gm/l for contact time 80 min. As the amount of catalyst increases, number of active sites of the catalyst increases, degradation of acid violet dye also increases is shown in the Fig. 7.

Effect of pH

The photocatalytic degradation of acid violet 19 dye is studied at different pH values as it is an important parameter for reaction taking place on the particular surface. The role of pH in photocatalytic degradation of dye is studied in the pH range 1–13 at dye concentration 20 mg/l and PANI–Fe_3O_4 amount 6 gm\l. It is observed that the rate of photocatalytic degradation enhanced with an increase in pH up to 7 and then decreased at higher pH as shown in the (Fig. 8). At higher pH, the amine sites of polyaniline chain were deprotonated and polyaniline did not prefer the adsorption of cationic acid violet 19 dye due to electrostatic repulsion, hence rate of photocatalytic degradation decreased. Similarly at lower pH, the amine group of acid violet 19 dye was protonated therefore it could not adsorbed on the surface of PANI with +ve charges. As the rate of adsorption decreases, therefore rate of photocatalytic degradation also decreases. As in this experiment dye is first adsorbed, and then photo catalytically degraded. This reveals that maximum rate of photocatalytic degradation was observed in neutral condition.

Effect of contact time

The effect of contact time for the photocatalytic degradation of acid violet 19 dye by PANI–Fe_3O_4 nanocomposite is shown in the (Fig. 9). The dye is rapidly degraded in 1st 20 min and then degradation rate increases slowly and reaches equilibrium in about 60 min. The rate of degradation of dye is initially fast because it has maximum number of active sites. As the maximum concentration of dye is degraded from aqueous solution the rate of degradation reaches at equilibrium in about 60 min. The degradation of dye at equilibrium decreases from 95.2 to 82.1 % as dye concentration is increased from 20 to 60 mg/l for 6 gm/l catalyst dose.

Kinetics study

Pseudo 1st Order

The photocatalytic degradation of acid violet 19 dye on the surface of PANI–Fe_3O_4, follows pseudo-first-order kinetics. It can be expressed as, where C and C_0 are the reactant concentration at time $t = t$ and $t = 0$, respectively, k and t are the pseudo-first-order rate constant (reaction rate constant) and time, respectively (Chen 2011). The relationships between [ln (C/C_0)] and irradiation time (reaction time) are as shown in the (Fig. 10). It is obvious that there exists a linear relationship between [ln (C/C_0)] and irradiation time. The pseudo-first-order rate constant k and linear

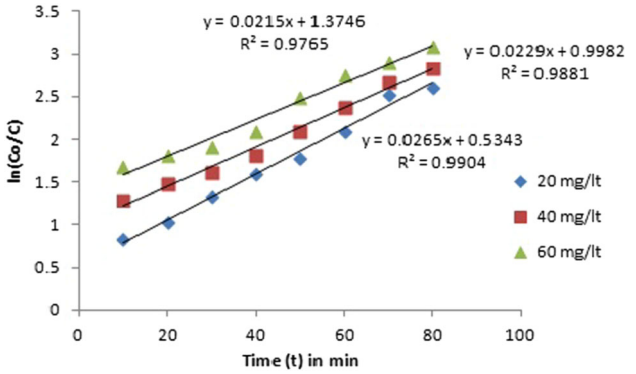

Fig. 10 Pseudo-first-order kinetics for photocatalytic degradation of acid violet dye with catalyst (PANI–Fe_3O_4) dose 6 gm/l

Table 1 Reaction rate constant of acid violet 19 photocatalytic degradation with different Initial concentration

Amount of catalyst	Conc. of dye in mg/l	Rate const. (K)	R^2
6 gm/l	20	0.0610	0.9904
	40	0.0229	0.9881
	60	0.0215	0.9765

regression coefficient (R^2) for acid violet 19 solutions with different initial acid violet 19 concentrations are summarized in Table 1, respectively. According to the Langmuir–Hinshelwood model, the fact that the decrease of reaction rate constant with the increase of the initial concentration of acid violet solutions obtained from Table 1 could be explained as follows. The acid violet dye is first adsorbed on the surface of PANI–Fe_3O_4, and then the photocatalytic degradation takes place under UV–Visible light irradiation. With the increase of the initial acid violet 19 concentrations, the acid violet molecules congregate on the surface of PANI–Fe_3O_4 catalysts. However, quenching between these excited molecules irradiated by UV–Visible light will take place. The quenching probability could also increase with the increase of the initial acid violet dye concentrations. Consequently, the photocatalytic efficiency (rate constant) of acid violet 19 solutions is decreased from 0.0610 to 0.0215 min^{-1} with the increase of the initial acid violet 19 concentrations from 20 to 60 mg/l.

Conclusions

1. PANI–Fe_3O_4 nanocomposite is successfully synthesised in situ through self polymerisation of monomer aniline.
2. Photocatalytic degradation of acid violet 19 dye using catalyst PANI–Fe_3O_4 is successfully carried. The photocatalytic degradation rate increased significantly by increasing amount of catalyst dose, while with an increasing dye concentration photocatalytic degradation rate decreases. Neutral (pH 7) condition is found, which significantly affects the degradation efficiency of acid violet 19 dye. The maximum degradation of acid violet 19 dye at pH = 7 is 95.2 % and after elution the concentration of dye is 20 mg/l.
3. The present study shows that conducting PANI–$NiFe_2O_4$ can be used as photo catalyst for the degradation of acid violet 19 dye from aqueous solution.
4. The rate of photo-degradation is found to confirm the pseudo-first-order kinetics with good correlation with R^2 values.

Acknowledgments Authors are gratefully acknowledged to the Director UDCT, Jalgaon (M.S) for SEM, EDS, FT-IR & XRD studies. Authors are also thankful to Director of IIT Madras for VSM studies. Authors are thankful to the Vice chancellor NMU Jalgaon for providing financial support under the VCRMS project and the Principal of G. T. Patil College, Nandurbar for providing necessary laboratory facilities.

References

Ameta R, Kumar D, Jhalora P (2014) Photocatalytic degradation of methylene blue using calcium oxide. Acta chim Pharma Indica 4(1):20–28

Aplin R, Waite TD (2003) Comparison of three advanced oxidation processes for degradation of textile dyes. Water Sci Tech 42:345–354

Chen C, Liu J, Liu P, Yu B (2011) Investigation of photocatalytic degradation of methyl orange by using nano-sized zno catalysts, advance. In Chem Eng Sci 1:9–14

Chatterji D (2004) Visible light induced photodegradation of organic pollutants on dye adsorbed TiO_2 surface. Bull Catal Soc Ind 3:56–58

Chen XY, Yu T, Gao F, Zhang HT, Liu LF, Wang YM, Li ZS, Zou ZG, Liu JM (2007) Application of weak ferromagnetic $BiFeO_3$ films as the photoelectrode materials under visible light irradiation. Appl Phys Lett 91:022114–022117

del Maria C, Cotto-Maddonado C, Campo Teresa, Arancha Eduardo Elizalde, Morant Carmen, marquez Francisco (2013) Photocatalytic degradation of Rhodamine-B under uv-visible light irradiation using different nanostructured catalyst, American. Chem Sci J 3(3):178–202

El-Mahy Safaa K, Dawy M, Abd El Aziz E (2013) Synthesis and electrical properties of polyaniline-Fe_3O_4 nanocomposite. J Appl Sci Res 9(4):2918–2926

Grätzel M (2004) Conversion of sunlight to electric power by nanocrystalline dye-sensitized solar cells. J Photochem Photobio A Chem 164:3–14

Houas A, Lachheb H, Ksibi M, Elaloui E, Guillard C, Herrmann J-M (2001) Photocatalytic degradation pathway of methylene blue in water. App Catal B Environ 31:145–157

Imanishi M, Hashimoto K, Kominami H (2010) Homogeneous photocatalytic mineralization of acetic acid in an aqueous solution of iron ion. Appl Catal B 97:213–219

Jang JS, Hong SJ, Lee JS (2009) Synthesis of zinc ferrite and its photocatalytic application under visible light. J Korean Phys Soc 54:204–208

Meshram S, Limaye R, Ghodke S, Nigam S, Sonawane S, Chikate R (2011) Continuous flow photocatalytic reactor using ZnO–bentonite nanocomposite for degradation of phenol. Chem Eng J 172:1008–1015

Patil Manohar R, Shrivastava VS (2014) Photocatalytic degradation of carcinogenic methylene blue dye by using polyaniline-nickel ferrite nano-composite. Der Chemica Sinica 5(2):8–17

Patil BN, Shirsath DS, Marathe YV, Shhrivastava VS (2012) Application of magnetic Nano adsorbent Fe_2O_3 for removal of hazardous Ponceau-s dye from aqueous solution. J App Chem Res 6(3):7–21

Sato J, Kobayashi H, Inoue Y (2004) Photocatalytic activity for water decomposition of RuO_2-dispersed Zn_2GeO_4 with d10 configuration. J Phys Chem B 108:4369–4375

Senadeera GKR, Kitamura T, Wada Y, Yanagida S (2004) Deposition of polyaniline via molecular self-assembly on TiO_2 and its uses as a sensitiser in solid-state solar cells. J Photochem Photobiol A164:61–66

Shrivastava VS (2012) Photocatalytic degradation of methylene blue and chromium metal from wastewater using nanocrystalline TiO2 semiconductor. Archieves of app Sci Res 4(3):1244–1254

Soltani T, Entezari MH (2013) Solar photocatalytic degradation of RB5 by ferrite bismuth nanoparticles synthesised via ultrasound. Ultrasonics Sonochem 20:1245–1253

Singhal S, Sharma R, Singh C, Bansal S (2013) Enhanced photocatalytic degradation of methylene blue using $ZnFe_2O_4$/MWCNT composite synthesised by hydrothermal method, India. J Mat Sci 2013:35625–35631

Tang JW, Zou ZG, Yin J, Ye JH (2003) Photocatalytic degradation of methylene blue on $Caln_2O_4$ under visible light irradiation. Chem Phys Lett 382:175–179

Wang W, Serp P, Kalck P, Faria IL (2005) "Visible light photodegradation of phenol on MWNT-TiO2 composite catalyst a prepared by a modified Sol–gel method. J Mole Catal A 235(1–2):194–199

Zhang H, Zong R, Zhao J, Zhu Y (2008) Dramatic visible photocatalytic degradation performances due to synergetic effect of TiO_2 with PANI. Environ Sci Technol 42:3803–3807